Depletion interactions in two-dimensional colloid–polymer mixtures: molecular dynamics simulations

2009 J. Phys.: Condens. Matter 21 035101

(http://iopscience.iop.org/0953-8984/21/3/035101)

J. Phys.: Condens. Matter **21** (2009) 035101 (7pp) doi:10.1088/0953-8984/21/3/035101

Depletion interactions in two-dimensional colloid–polymer mixtures: molecular dynamics simulations

Soon-Chul Kim[1], **Baek-Seok Seong**[2] **and Soong-Hyuck Suh**[3]

[1] Department of Physics, Andong National University, Andong 760-749, Korea
[2] HANARO Center, KAERI PO Box 105, Yuseong, Daejeon 305-600, Korea
[3] Department of Chemical Engineering, Keimyung University, Taegu 704-701, Korea

E-mail: sckim@andong.ac.kr and shsuh@kmu.ac.kr

Received 30 June 2008, in final form 27 October 2008
Published 10 December 2008
Online at stacks.iop.org/JPhysCM/21/035101

Abstract
The depletion interactions acting between two hard colloids immersed in a bath of polymers, in which the interaction potentials include the soft repulsion/attraction, are extensively studied by using the molecular dynamics simulations. The collision frequencies and collision angle distributions for both incidental and reflection conditions are computed to study the dynamic properties of the colloidal mixtures. The depletion effect induced by the polymer–polymer and colloid–polymer interactions are investigated as well as the size ratio of the colloid and polymer. The simulated results show that the strong depletion interaction between two hard colloids appears for the highly asymmetric hard-disc mixtures. The attractive depletion force at contact becomes deeper and the repulsive barrier becomes wider as the asymmetry in size ratio increases. The strong polymer–polymer attraction leads to the purely attractive depletion interaction between two hard colloids, whereas the purely repulsive depletion interaction is induced by the strong colloid–polymer attraction.

1. Introduction

The phase behaviors of colloids in a molecular solution have recently been the subject of many theoretical and experimental studies because of the various biological and industrial applications. However, determining the structure and phase behaviors of colloids in a molecular solution is a tough problem because of the complexity of colloid–polymer mixtures [1]. Colloidal suspensions, such as paints, glue, inks, etc, exhibit interesting transport and structural properties and a great variety of thermodynamic phases depending on size, shape and concentration of their constituents. The potential range for the aggregation of colloidal suspensions can change either the aggregated shape and the aggregation kinetics, and can have a strong influence both on the equilibrium structure and on their growth kinetics [2, 3].

In performing the experiment with colloidal suspensions, one usually focuses attention on the colloidal particles only. The experimental data can be interpreted by means of an effective interaction between the colloids, which indirectly includes all of the effects of the remaining constituents; the colloids in a polymer solution can be expressed as one-component colloids with the effective interaction [1]. The effective interactions are a power tool to extract macroscopic properties of colloids from microscopic details. This has stimulated a growing interest in ascertaining quantitative details of the depletion interactions. It is known that the additions of the repulsive/attractive interactions beyond the hard core may profoundly influence the structural properties and phase behaviors of systems as well as the potential range and shape of the colloidal suspensions does [3]. Indeed, the depletion forces can be strongly affected if the attractive or repulsive interactions are present in the system.

Many theoretical approaches, which are based on the integral equation theory [4–7] and the density functional theory [8–12], have been proposed for studying the depletion interactions along with the computer simulations [5–8, 13]. Each approach has some advantages and disadvantages in actual applications. In principle, the structure of complex physical systems can be computed to arbitrary accuracy through computer simulations, even though it needs more computational time compared with the theoretical approaches.

Computer simulations for the depletion interaction in the various systems have also been performed rather extensively. Nevertheless, many studies are restricted to three-dimensional systems such as the large spheres immersed in a multi-component mixture of small spheres [8, 13] or the polymer chain solutions [14], but not to two-dimensional systems with the repulsive/attractive interactions beyond the hard core [5]. A little is known about the depletion effect induced by the intermolecular potentials of particles as well as the size ratio of particles composed of a system. Furthermore recent progress in the experimental technique made it possible to confine colloids to two [15] and even one dimension [16] and to observe particle trajectories with video microscopy.

In this paper, we present extensive results, based on the molecular dynamics (MD) simulations, for the depletion interactions between two hard colloids induced by the polymer–polymer and colloid–polymer interactions with the soft repulsive/attractive potential. In section 2, the simulation models including the MD simulations have been described in detail. In section 3, the simulated results have been compared with the theoretical approaches such as the nonlinear integral equations and fundamental-measure theory [17]. The collision frequencies and collision angle distributions by the hard polymer are computed to investigate the dynamic properties of the colloidal mixtures. The depletion interaction acting between two colloids induced by the polymer–polymer and colloid–polymer interactions has been analyzed as well as the size ratio of the colloid and polymer composed of a system. Finally, the paper ends with a section of concluding remarks.

2. Simulation models

2.1. Model potentials

We consider two hard colloids (species c) immersed in a suspension of polymers (species p) with the soft repulsive/attractive step interactions. In this case, the intermolecular interaction $\phi_{cc}(r)$ between two hard colloids is assumed as the hard-disc interaction

$$\phi_{cc}(r) = \begin{cases} \infty, & r < \sigma_c \\ 0, & \text{otherwise}, \end{cases} \tag{1}$$

where σ_c is the diameter of a hard colloid. The colloid–polymer interaction $\phi_{cp}(r)$ between colloid and polymer is defined by

$$\phi_{cp}(r) = \begin{cases} \infty, & r < \sigma_{cp} \\ \epsilon_{cp}, & \sigma_{cp} < r < \sigma_{cp} + \delta_{cp} \\ 0, & \text{otherwise}, \end{cases} \tag{2}$$

where $\sigma_{cp} = (\sigma_c + \sigma_p)/2$ is the hard-core diameter, δ_{cp} the width of the repulsive/attractive step, and ϵ_{cp} its height representing the strength of repulsion/attraction. The polymer–polymer interaction $\phi_{pp}(r)$ is defined by

$$\phi_{pp}(r) = \begin{cases} \infty, & r < \sigma_p \\ \epsilon_{pp}, & \sigma_p < r < \sigma_p + \delta_{pp} \\ 0, & \text{otherwise}, \end{cases} \tag{3}$$

where σ_p is the diameter of a polymer modeled as a hard disc with the soft repulsive/attractive step ϵ_{pp} and strength δ_{pp}. In this model, $\epsilon_{ij} = 0$ means two hard colloids in a bath of hard discs. For $\epsilon_{ij} < 0$, the model is reduced to the square-well disc that consists of a hard-disc repulsion plus an attractive square well. This model has two intrinsic length scales. The ratio of these lengths determines the phase behaviors [3]. For $\epsilon_{ij} > 0$, this model becomes hard discs with the soft repulsion (square-shoulder potential). A number of physical systems are characterized by the presence of a penetrable corona surrounding a substantially impenetrable core. Such core–corona molecule architectures are modeled by the square-shoulder system. This system shows the isostructural solid–solid transition and the melting-curve extreme [18].

2.2. Molecular dynamics (MD) simulations

Our simulation set-up contains two hard colloids in a large square box of length $L = 40\sigma_p$ with periodic boundary conditions in all directions. During MD simulations two hard colloids having the diameter σ_c remain fixed in their positions along with the diagonal direction with separation distance r. The MD simulations were conducted in a manner similar to that described by Alder and Wainwright for hard-core systems [19]. For the MD simulations, the initial velocities of the particles were randomly chosen from the equilibrium Maxwell–Boltzmann distribution function. 500 collisions per particle were attempted to generate a set of equilibrium positions at a given density, and the depletion force was determined during an additional 5000 collisions per particle. The simulated depletion force acting on the two hard colloids is computed by summing the linear moment exchanges over all collisions between the polymer and the hard colloids. Those collisional moment vectors are projected onto the particle separation vector such that a positive sign means repulsion. The corresponding depletion potential, at a given condition of the size ratio and the packing fraction, is accessed as a function of r by integrating the distances-resolved simulation force. Collision frequencies and collision angle distributions for both incidental and reflection conditions are computed to investigate the dynamic properties of such two-dimensional colloidal mixtures. The diameter of a hard polymer σ_p has been chosen as the unit through the numerical calculation.

3. Results and discussion

3.1. Effects of polymer–polymer interactions

The simulated depletion forces $\beta f^{dp}(r)\sigma_p$ induced by the polymers (hard discs) with diameter σ_p in the infinite dilute limit of the colloids (hard discs) with diameter σ_c ($\sigma_c > \sigma_p$) are presented in figure 1, where the bulk densities of polymers are $\rho_p\sigma_p^2 = 0.2$ and 0.4, and the size ratio $\varphi \equiv \sigma_c/\sigma_p = 5$ and 10. Figure 1 shows an attractive force when two hard colloids are separated by a small distance ($\sigma_c < r < \sigma_c + \sigma_p/2$), due to the depletion effect. The strong repulsive peak appearing at $r = \sigma_c + \sigma_p$ is due to the large concentrative gradients of polymers composed of the small hard discs inside the gap

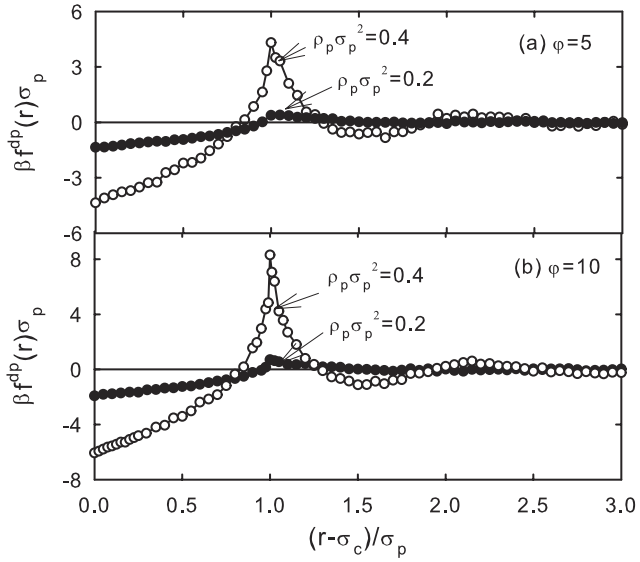

Figure 1. (a) Depletion forces $\beta f^{\rm dp}(r)\sigma_{\rm p}$ induced by the hard discs ($\varphi = 5$). The curve is just a guide for the eye. (b) $\varphi = 10$.

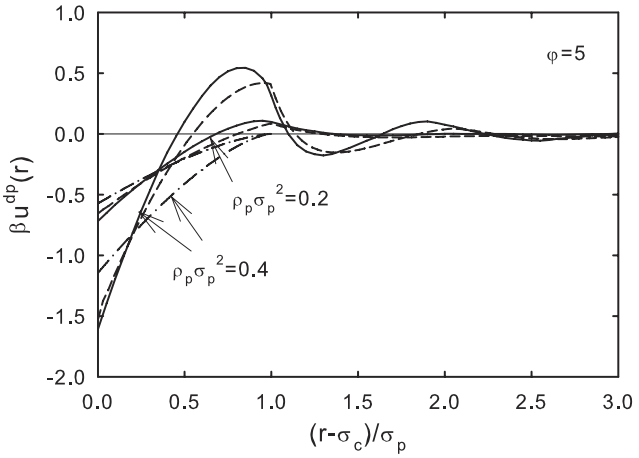

Figure 2. Depletion potential $\beta u^{\rm dp}(r)$ induced by the hard discs: solid lines (computer simulations), dotted–dashed lines (AO potential [5]) and dashed lines (MFMT theory [17]).

between two hard colloids. With increasing bulk density of the polymers, both the attractive and repulsive forces become stronger. In this case, their interactions are due to the exclusion of volume types. We can check that our simulated depletion forces compare very well with those of Castaneda-Priego *et al* [5, 6].

The depletion potential $\beta u^{\rm dp}(r)$ calculated from the MD simulations is displayed in figure 2 along with the results of the Asakura–Oosawa (AO) potential [5, 6] and the modified fundamental-measure theory (MFMT) proposed by Kim *et al* [17], where the depletion potential $\beta u^{\rm dp}(r)$ is related to the depletion force $\beta f^{\rm dp}(r)$ such as

$$\beta u^{dp}(r) = -\int_r^\infty {\rm d}s\, \beta f^{\rm dp}(s). \tag{4}$$

The trapezoidal method with $\Delta r = 0.01\sigma_{\rm p}$–$0.02\sigma_{\rm p}$ has been used to calculate the depletion potentials for the range of r–$\sigma_{\rm c} = 6\sigma_{\rm p}$–$8\sigma_{\rm p}$ numerically.

The AO potential [5, 6], which is based on the first-order approximation in the density expansion with respect to the density of the hard polymers, is given by

$$\beta u^{\rm AO}(r) = -\frac{2\rho_{\rm p}\sigma_{\rm p}^2}{\pi}(1+\varphi)^2\left[\cos^{-1}\left(\frac{1}{1+\varphi}\frac{r}{\sigma_{\rm p}}\right) - \left(\frac{1}{1+\varphi}\frac{r}{\sigma_{\rm p}}\right)\sqrt{1-\left(\frac{1}{1+\varphi}\frac{r}{\sigma_{\rm p}}\right)^2}\right] \tag{5}$$

for $\sigma_{\rm c} \leqslant r \leqslant \sigma_{\rm c} + \sigma_{\rm p}$ and 0 for larger distances. It is noted here that the AO interaction is purely attractive. At the low polymer density $\rho_{\rm p}\sigma_{\rm p}^2 = 0.2$, the AO potential $\beta u^{\rm AO}(r)$ is shown to be in good agreement with computer simulation results. However, the larger deteriorations at contact ($r = \sigma_{\rm c}$) and near the repulsive barrier ($r = \sigma_{\rm c} + \sigma_{\rm p}$) are found for the higher polymer density $\rho_{\rm p}\sigma_{\rm p}^2 = 0.4$, while the MFMT [17] compares well with the computer simulations and is better than the nonlinear integral equations based on the Percus–Yevick (PY) and Rogers–Young (RY) [20] closure relations, even though we did not display the PY and RY results [5] in the figures. At the high polymer density, the MFMT approach slightly underestimates the repulsive barrier. Perhaps the discrepancy between the MFMT approach and the computer simulation comes from the fact that in two dimensions the Mayer f bond cannot be deconvoluted exactly with a finite number of weight functions [10, 17, 21]. It is expected that the cusp effect appears approximately at a distance $r \approx \sigma_{\rm c} + \sigma_{\rm p}$. Actually, the particle density distributions $\rho_{\rm p}(r)\sigma_{\rm p}^2$ for the hard discs confined in a hard circular cavity systematically overemphasize the cusp at $r = \sigma_{\rm p}$ away from the hard wall [17]. Figures 1 and 2 indicate that the strong depletion interaction appears for the highly asymmetric hard-disc mixtures. On the other hand, the depletion potential $\beta u^{\rm dp}(r = \sigma_{\rm c})$ at contact can be estimated from the contact value of the radial distribution function $g_{\rm cc}(r)$ of the hard colloids such as

$$\beta u^{\rm dp}(r = \sigma_{\rm c}) = -\ln g_{\rm cc}(r = \sigma_{\rm c}), \tag{6}$$

where $g_{\rm cc}(r = \sigma_{\rm c})$ denotes the radial distribution function of the hard colloids at contact. The semi-empirical expression [22], where the contact radial distribution function of the hard-disc mixtures is well known, yields the depletion potential at contact

$$\beta u^{\rm dp}_{\rm semiemp}(r = \sigma_{\rm c}) = -\ln\left[\frac{1}{1-n_2} + \frac{9}{64}\frac{n_1\sigma_{\rm p}}{(1-n_2)^2}\right] \tag{7}$$

with $n_1 = \pi\rho_{\rm p}\sigma_{\rm p}$ and $n_2 = \pi\rho_{\rm p}\sigma_{\rm p}^2/4$. The calculated depletion potentials at contact for $\varphi = 2$ and 5 compare with the computer simulations in figure 3. Figure 3 shows that the MFMT theory [17] is better than the AO approximation and compares well with the simulated results. This result suggests that the MFMT approach based on the test-particle method of Percus yields an accurate contact radial distribution function of hard-disc mixtures [17].

In figure 4, the incidental/reflection collision angle distributions by the hard polymers are displayed, which are

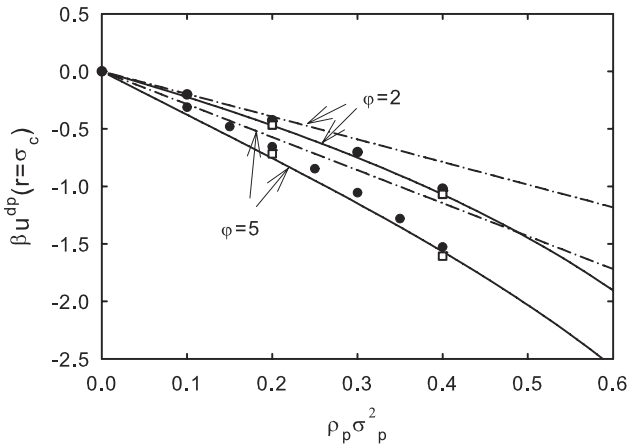

Figure 3. Depletion potential $\beta u^{\rm dp}(r=\sigma_{\rm c})$ as a function of polymer density $\rho_{\rm p}\sigma_{\rm p}^2$. The solid and dotted–dashed lines are the results of equation (7) based on the semi-empirical equation of the contact value and the AO potential, respectively. The solid circles and open squares are from the MFMT approach and the computer simulations.

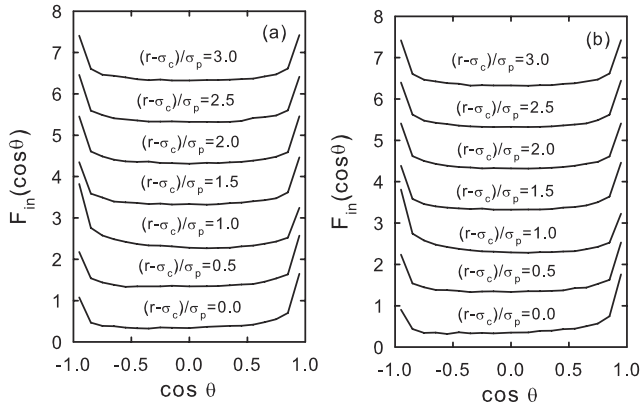

Figure 4. (a) Incidental collision angle distribution $F_{\rm in}(\cos\theta)$ for the hard discs ($\rho_{\rm p}\sigma_{\rm p}^2 = 0.4$ and $\varphi = 5$). Results for $F_{\rm in}(\cos\theta)$ are shifted upwards by one unit for clarity. (b) $\rho_{\rm p}\sigma_{\rm p}^2 = 0.4$ and $\varphi = 10$.

defined by the cosine of the incidental/reflection angle between the collisional velocity vector and the relative position vector of two stationary colloid particles

$$F_{\rm in}(\cos\theta) = \frac{f_{\rm in}(\cos\theta)}{\int_{-1}^{1} f_{\rm in}(\cos\theta)\mathrm{d}\cos\theta} \qquad \text{and}$$
$$F_{\rm re}(\cos\theta) = \frac{f_{\rm re}(\cos\theta)}{\int_{-1}^{1} f_{\rm re}(\cos\theta)\mathrm{d}\cos\theta}, \tag{8}$$

where $f_{\rm in}(\cos\theta)$ and $f_{\rm re}(\cos\theta)$ denote the incidental and reflection collision angle frequency at $\cos\theta$, respectively. The incidental collision angle distributions satisfies $F_{\rm in}(\cos\theta) = F_{\rm re}(\cos(-\theta))$ by the symmetric property. For the system of $r-\sigma_{\rm c}/\sigma_{\rm p} = 0$, $F_{\rm in}(\cos\theta)$ shows the maximum value at $\cos\theta = 1$. $F_{\rm in}(\cos\theta)$ at $\cos\theta = 1$ decreases with increasing distance between two hard colloids, whereas $F_{\rm in}(\cos\theta)$ at $\cos\theta = -1$ relatively increases. For the system of $r - \sigma_{\rm c}/\sigma_{\rm p} = 1.0$, $F_{\rm in}(\cos\theta = -1)$ approaches the maximum value. Finally, $F_{\rm in}(\cos\theta)$ satisfies $F_{\rm in}(\cos\theta = 1) = F_{\rm in}(\cos\theta = -1)$

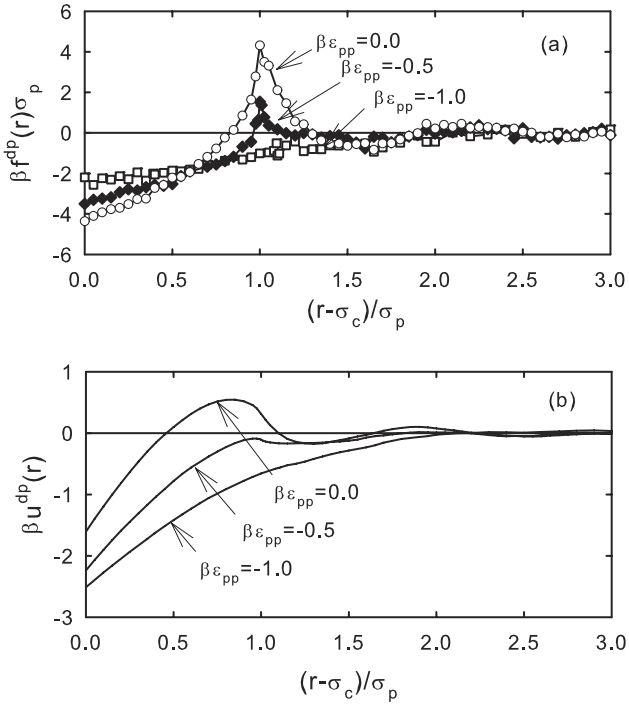

Figure 5. (a) Depletion forces and (b) potentials induced by the polymer–polymer attraction ($\delta_{\rm pp} = 0.5$ and $\varphi = 5$).

at large distances greater than $r - \sigma_{\rm c} = 3\sigma_{\rm p}$. The large differences between two collision angle distributions, $|\int_0^1 F_{\rm in}(\cos\theta)\mathrm{d}\cos\theta - \int_0^{-1} F_{\rm in}(\cos\theta)\mathrm{d}\cos\theta|$, are found at $(r-\sigma_{\rm c})/\sigma_{\rm p} = 0$ and $(r-\sigma_{\rm c})/\sigma_{\rm p} = 1$, which correspond to the strong attractive and repulsive interaction. This means that the incidental/reflection collision angle distributions depend on the local polymer density distribution inside the gap between two hard colloids. The collision frequency (the linear moment exchanges over all collisions between the polymer and the hard colloids) is proportional to the local polymer density inside the gap between two hard colloids. Thus, we can conclude that the repulsive (or attractive) interaction between two hard colloids appears when the local polymer density inside the gap between two hard colloids is larger (or smaller) than the bulk polymer density.

In figure 5, we present the depletion interactions between two hard colloids induced by the polymer–polymer attraction, where the colloid–polymer interaction is assumed as the purely hard repulsion with $\beta\epsilon_{\rm cp} = 0$. The attractive force at contact and repulsive force at $r = \sigma_{\rm c} + \sigma_{\rm p}$ become weaker with increasing polymer–polymer attraction. At large distance, the oscillatory behavior has disappeared. Finally, the purely attractive depletion force increases the purely attractive depletion potential $\beta u^{\rm dp}(r)$ between two hard colloids; the depletion potential becomes purely attractive and decays monotonically. This implies that the polymers cannot easily penetrate inside the gap between two hard colloids because of the attraction between polymers; the polymers with the square-well attraction behave like the polymer chains which are weakly connected. The recent simulated results [14, 23] also demonstrate that the polymer chain cannot easily penetrate

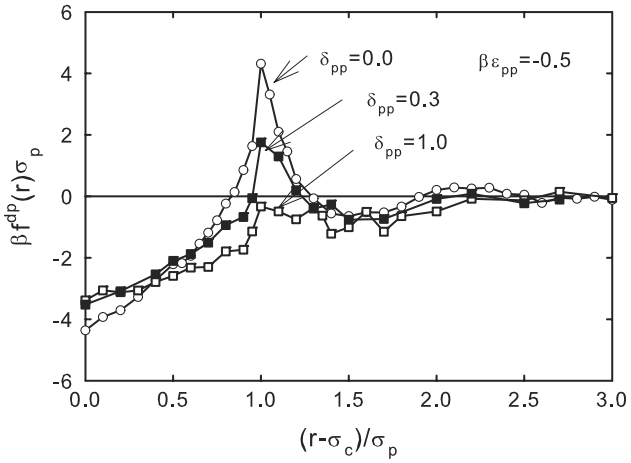

Figure 6. Depletion forces induced by the polymer–polymer attraction ($\varphi = 5$).

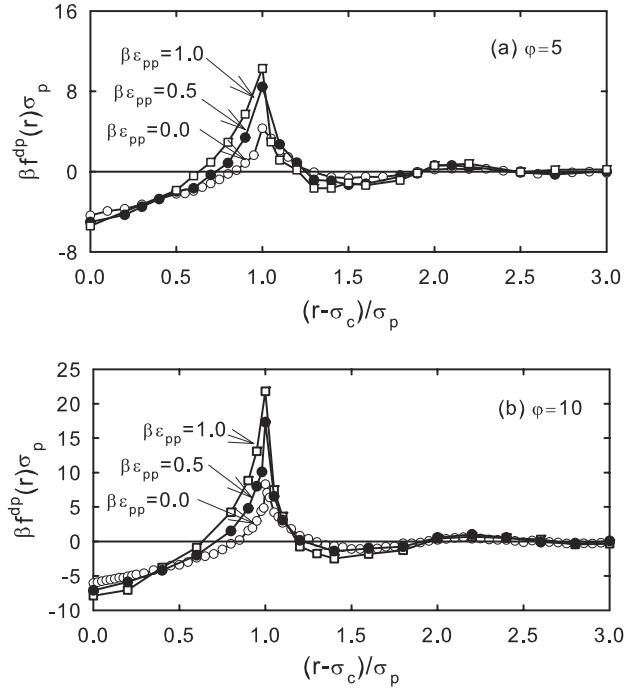

Figure 7. Depletion forces induced by the polymer–polymer repulsion with $\delta_{pp} = 0.5$.

inside the gap between two hard colloids compared with the hard spheres with the purely repulsive interaction. This result also indicates the importance of the polymer density in the gap between two colloids. Thus, in the case of the strong polymer–polymer attraction, the repulsive barrier is not observed due to the small concentration gradients of the polymers inside the gap between two hard colloids. The calculated depletion interactions as a function of the step width δ_{pp} are presented in figure 6 for $\beta\epsilon_{pp} = -0.5$. As expected from figure 5, the attractive interaction is found for the wide step width because of the strong polymer–polymer attraction. The depletion interaction becomes more attractive with increasing step width δ_{pp} and the oscillation at large distance decays monotonically.

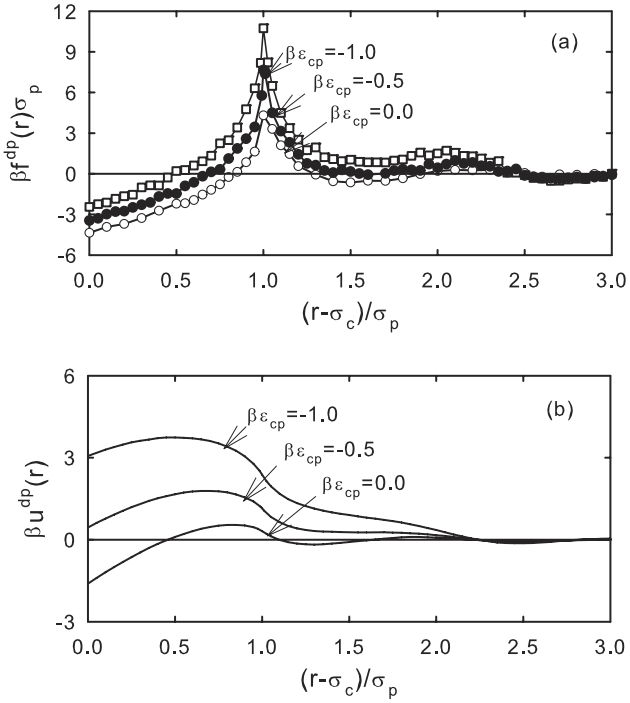

Figure 8. (a) Depletion forces induced by the colloid–polymer attraction ($\delta_{cp} = 0.5$ and $\varphi = 5$). (b) Depletion potentials.

The depletion forces between two hard colloids induced by the polymer–polymer repulsion are depicted in figure 7, where the width of the repulsive step is $\delta_{pp} = 0.5$. Comparison with figure 1 shows that, with increasing polymer–polymer repulsion, the depletion interaction at contact is more attractive and the oscillation is more long-ranged compared with that of the hard-disc mixtures. The strong depletion interaction appears for the highly asymmetric colloid–polymer mixtures, as can be expected from figure 1. This means that the polymer–polymer repulsion does not create the purely repulsive depletion interaction. One can here conclude that the purely attractive depletion force between two hard colloids is induced by the strong polymer–polymer attraction, whereas the polymer–polymer repulsion leads to strong oscillatory behaviors for the depletion interactions.

3.2. Effects of colloid–polymer interactions

We consider the effect of colloid–polymer interaction, which is given by the soft attractive/repulsive interaction, for the depletion forces acting between two hard colloids. The depletion forces and potentials induced by the colloid–polymer attraction are displayed in figures 8 and 9, where the polymer–polymer interaction is assumed as the hard repulsion with $\beta\epsilon_{pp} = 0$. With increasing colloid–polymer attraction, the depletion force at contact becomes weaker, whereas the repulsive maximum at $r = \sigma_c + \sigma_p$ becomes much stronger and the repulsive barrier becomes much wider. Finally, it leads to the long-ranged repulsive potentials. In particular, the position of the first repulsive potential barrier shifts to shorter distances until it reaches a new stable position at $r \sim \sigma_c + \sigma_p/2$. This result illustrates that the polymers modeled as hard discs

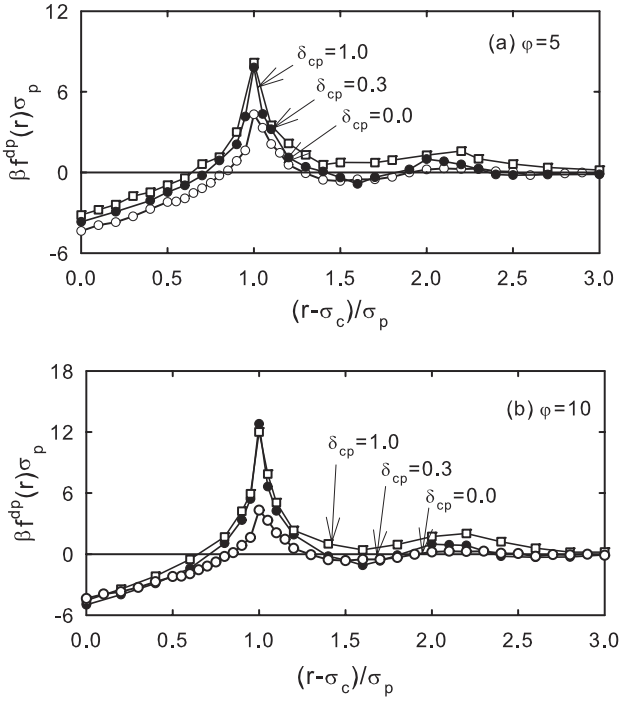

Figure 9. Depletion forces induced by the colloid–polymer attraction with $\beta\epsilon_{cp} = -0.5$.

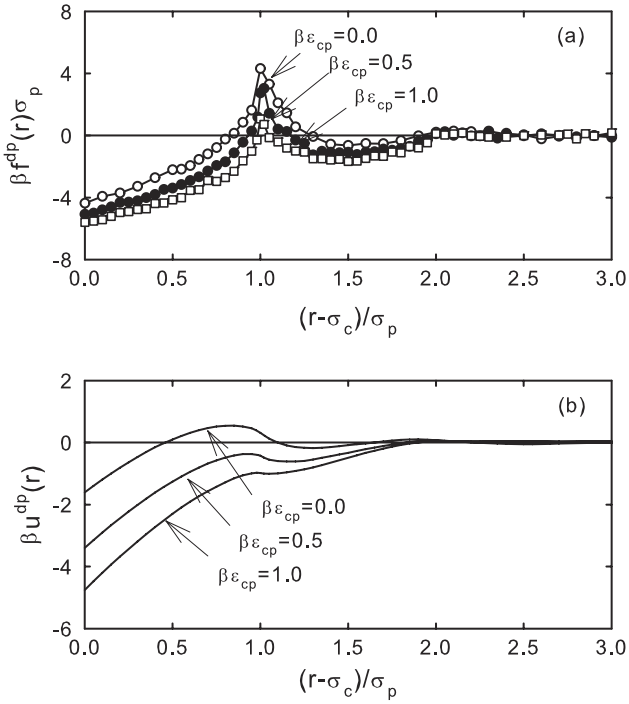

Figure 10. (a) Depletion forces induced by the colloid–polymer repulsion ($\delta_{cp} = 0.5$ and $\varphi = 5$). (b) Depletion potentials.

can easily penetrate inside the gap between two hard colloids compared with those of hard discs because of the colloid–polymer attraction. The local polymer density inside the gap between two colloids is relatively larger than the bulk polymer density. The large polymer density inside the gap leads to the weak attraction at contact and the strong repulsive interaction at $r = \sigma_c + \sigma_p$. Figure 9 shows the effect of colloid–polymer attraction for two different size ratios φ, where $\varphi = 5$ and 10. The attractive interaction at contact becomes stronger and the repulsive barrier becomes wider as the asymmetry in size ratio increases. The large size ratio develops the strong oscillatory interaction compared with those of the small size ratio.

The effect of colloid–polymer repulsion for the depletion interaction is presented in figure 10, where $\delta_{cp} = 0.5$ and $\varphi = 0.5$. It shows that the colloid–polymer repulsion leads to the weak depletion interaction. With increasing colloid–polymer repulsion, the depletion interaction at contact becomes more attractive because of the colloid–polymer repulsion. For the strong colloid–polymer repulsion, the depletion interaction becomes purely attractive. This leads to the purely attractive potential $\beta u^{dp}(r)$; the position of the first repulsive barrier shifts to large distances as expected from figure 5. The overall picture shows that the polymer–polymer attraction leads to the weak attraction as does the colloid–polymer repulsion. The strong polymer–polymer attraction and colloid–polymer repulsion lead to the purely attractive potential between two hard colloids, whereas the strong colloid–polymer attraction induces the purely repulsive potential. This result explains that the colloid–polymer repulsion relatively decreases the average polymer density inside the gap between two hard colloids compared with that of the hard discs. Finally, we have shown the depletion interactions induced by the colloid–polymer and polymer–polymer interactions in figure 11. As expected from figures 4–11, it shows that the competition between the colloid–polymer interaction and the polymer–polymer interaction determines the depletion interaction between two hard colloids.

4. Conclusions

We have carried out MD simulations to study the depletion interaction acting between two hard colloids in a bath of the polymer with the attractive/repulsive interaction. The collision angle distributions by the hard polymers indicate that the attractive/repulsive interaction is related to the local polymer density inside the gap between two hard colloids. The calculated results show that the MFMT based on the test-particle theory of Percus yields an accurate depletion interaction compared with the PY and RY approximations, and compares well with the computer simulations. The competition between the colloid–polymer interaction and the polymer–polymer interaction determines the depletion interaction between two hard colloids as well as the size ratio in the colloid–polymer mixtures.

It would be very interesting to apply the depletion interaction to study the structure and phase behaviors of the two-dimensional colloids immersed in polymer solutions. This knowledge is essential in various areas of nanotechnologies in the particle–polymer system, and permits a systematic evaluation of the impact of size and shape parameters on the structure and thermodynamic properties of nanostructured colloids. It is also expected that the depletion interaction will provide a clue for investigating the fluid–fluid demixing

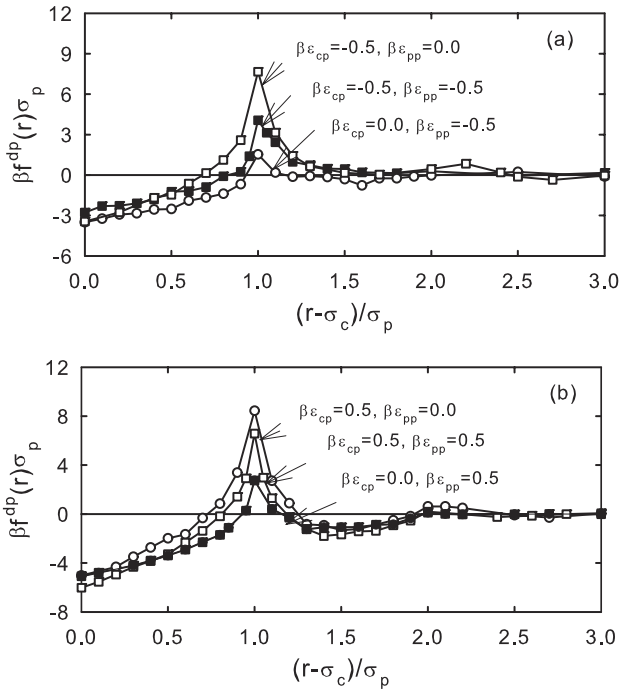

Figure 11. (a) Depletion forces induced by the polymer–polymer and colloid–polymer attractions ($\delta_{cp} = \delta_{pp} = 0.5$ and $\varphi = 5$). (b) Depletion forces induced by the polymer–polymer and colloid–polymer repulsions ($\delta_{cp} = \delta_{pp} = 0.5$ and $\varphi = 5$).

transition (fluid–fluid separation) for the highly asymmetric colloid–polymer mixture, which is still an open question. In the near future, we will investigate the structure and phase behaviors of the colloid–polymer mixture with the depletion interactions in order to devise an improved version of theoretical predictions for such systems.

Acknowledgments

This work was supported by the HANARO Center of KAERI and MOST, Korea Government, through the National Nuclear Technology Program.

References

[1] Likos C N 2001 *Phys. Rep.* **348** 267
[2] Videcoq A, Han M, Abélard P, Pagnoux C, Rossignol F and Ferrando R 2006 *Physica* A **374** 507
[3] Malescio G 2007 *J. Phys.: Condens. Matter* **19** 073101
[4] Méndez-Alcaráz J M and Klein R 2000 *Phys. Rev.* E **61** 4095
[5] Castaneda-Priego R, Rodriguez-López A and Méndez-Alcaraz J M 2003 *J. Phys.: Condens. Matter* **15** S3393
[6] Castaneda-Priego R, Rodriguez-López A and Méndez-Alcaraz J M 2006 *Phys. Rev.* E **73** 051404
[7] Guzman O and de Pablo J J 2003 *J. Chem. Phys.* **118** 2392
[8] Dijkstra M, vanRoij R and Evans R 1998 *Phys. Rev. Lett.* **81** 2268
Dijkstra M, vanRoij R and Evans R 1999 *Phys. Rev. Lett.* **82** 117
[9] Patel N and Egorov S A 2005 *J. Chem. Phys.* **123** 144916
Egorov S A 2005 *Phys. Rev.* E **72** 010401(R)
[10] Roth R and König P-M 2005 *Pramana J. Phys.* **64** 971
[11] Roth R and Kinoshita M 2006 *J. Chem. Phys.* **125** 084910
[12] Kim S-C, Suh S-H and Seong B-S 2007 *J. Chem. Phys.* **127** 114903
[13] Biben T, Bladon P and Frenkel D 1996 *J. Phys.: Condens. Matter* **8** 10799
[14] Striolo A, Colina C M, Gubbins K E, Elvassore N and Lue L 2004 *Mol. Simul.* **30** 437
[15] Brunner M, Bechinger C, Strepp W, Lobaskin V and von Grünberg H H 2002 *Europhys. Lett.* **58** 926
[16] Lutz C, Kollmann M and Bechinger C 2004 *Phys. Rev. Lett.* **93** 026001
[17] Kim S-C, Suh S-H and Seong B-S 2008 *Fluid Phase Equilib.* **268** 114
[18] Young D A and Alder B J 1977 *Phys. Rev. Lett.* **38** 1213
[19] Alder B J and Wainwright T E 1959 *J. Chem. Phys.* **31** 459
Allen M P and Tildesley D J 1987 *Computer Simulation of Liquids* (Oxford: Clarendon)
[20] Rogers F J and Young D A 1984 *Phys. Rev.* A **30** 999
[21] Rosenfeld Y 1990 *Phys. Rev.* A **42** 5978
Rosenfeld Y, Schmidt M, Löwen H and Tarazona P 1997 *Phys. Rev.* E **55** 4245
[22] Jenkins J T and Mancini F 1987 *J. Appl. Mech.* **54** 27
Barrio C and Solana J R 2001 *J. Chem. Phys.* **115** 7123
Barrio C and Solana J R 2002 *J. Chem. Phys.* **117** 2451
Barrio C and Solana J R 2006 *Fluid Phase Equilib.* **239** 46
[23] Goel T, Patra C N, Ghosh S K and Mukherjee T 2004 *J. Chem. Phys.* **121** 4865